TWO-STEP ESPRIT WITH COMPENSATION FOR MODELLING ERRORS USING A SPARSE CALIBRATION GRID

*Astrid Lundgren, Maria Lanne** *and Mats Viberg*

Chalmers University of Technology
Department of Signals and Systems
Gothenburg, Sweden

ABSTRACT

In arrays with scan dependent errors, such as large position errors, a dense calibration grid can become necessary. Calibration time is, however, very expensive and keeping the measured calibration grid as sparse as possible is important. In this paper it is shown how interpolation using local models can be used to make the calibration grid more dense without increasing the number of measurements. Furthermore, it is shown how the performance of the DOA estimation with ESPRIT using arrays with large position errors can be improved by a second step including weighted calibration.

***Index Terms*—** Antenna arrays, calibration, interpolation, direction of arrival estimation

1. INTRODUCTION

An array antenna is often modelled as being uniform and linear, but in reality it consists of many components which all have a limited manufacturing accuracy. This causes the signal paths from the antenna elements to differ from the ideal both in amplitude and phase. In addition to this, due to mutual coupling between the antenna elements, the signals will also depend on the position of the antenna element within the array.

To deal with imperfections in the array, a calibration is often necessary. Many calibration methods are global, which means that the same calibration is used for all Directions Of Arrival (DOA). This is sufficient if the imperfections only give rise to scan independent errors. Unfortunately some imperfections might cause scan dependent errors, like position errors and differences in element patterns, which can result in poor results from a global calibration.

Today most arrays are manufactured with a high mechanical and electrical accuracy, and the errors are small. But relaxing these requirements, might make the manufacturing process less costly. On the other hand, scan dependent errors require a more dense calibration grid, which is time consuming and expensive. Therefore, it is very important to use the calibration data in an efficient way to keep the number of calibration measurements to a minimum.

Previously, we have shown that the performance of DOA estimation using MUSIC for an array with scan dependent errors can be improved using local calibration, see [1]. Local calibration is easily applied to MUSIC. To apply local calibration to ESPRIT is, however, less straightforward. This paper studies ESPRIT and suggests two ways to improve the performance using local models. The first, which also can be applied to other DOA-estimation methods, is to make the calibration grid more dense by calculating pseudo calibration data though interpolation from the measured calibration data using local models. This reduce the need for calibration measurements. We will also show how the impact of scan dependent errors in DOA estimation using ESPRIT can be reduced by a two-step procedure involving a weighting of the calibration data.

In this paper vectors are written in bold lower case letters, and matrices in bold upper case letters. The transpose of a vector $\mathbf{a}$ is marked $\mathbf{a}^T$ while the complex conjugate transpose is marked $\mathbf{a}^*$.

(*)Also with Saab Microwave Systems, Gothenburg, Sweden

2. BACKGROUND

If d signals given by the vector $\mathbf{s}(t)$ arrive at an array from directions $\boldsymbol{\theta}$, the output from the array $\mathbf{x}(t)$ can be modelled as

$$\mathbf{x}(t) = \mathbf{A}(\boldsymbol{\theta})\mathbf{s}(t) + \boldsymbol{\eta}(t), \tag{1}$$

where $\boldsymbol{\eta}(t)$ is noise with variance σ^2 and $\mathbf{A}(\boldsymbol{\theta})$ is a matrix with the steering vectors. The steering vectors for a ULA are given by

$$\mathbf{a}(\theta) = [1, e^{j\Delta k \sin(\theta)}, ..., e^{j\Delta k \sin(\theta)(m-1)}]^T, \tag{2}$$

where Δ is the distance between the sensors, m is the number of sensors and $k = 2\pi/\lambda$ where λ is the wavelength of $\mathbf{s}(t)$. Assuming N time samples, an estimate of the covariance matrix $\mathbf{R}$ is calculated as a time average

$$\hat{\mathbf{R}} = \frac{1}{N}\sum_{t=1}^{N} \mathbf{x}(t)\mathbf{x}^*(t). \tag{3}$$

The data model in (1) is, however, a bit too simple to work for a real array, since there is no way to describe the imperfections or differences within the array. The ideal steering vector $\mathbf{a}(\theta)$ is therefore replaced by a real steering vector $\mathbf{a_{mod}}(\theta)$ including the imperfections. It is given by

$$\mathbf{a_{mod}}(\theta) = \mathbf{Q}\mathbf{a}(\theta), \tag{4}$$

where $\mathbf{Q}$ is a correction matrix. The purpose of the calibration is to find the true steering vectors $\mathbf{a_{mod}}(\theta)$, or in other words, the correction matrix $\mathbf{Q}$.

The calibration is performed in the following way. First calibration data is collected. One transmitter is used and moved in a grid of calibration angles $\boldsymbol{\theta}_{cal} = [\theta_{cal1}, \ldots, \theta_{calj}, \ldots, \theta_{calJ}]$, where J is the number of calibration angles. For each angle a steering vector $\hat{\mathbf{a}}_{\mathbf{meas}}(\theta_{calj})$ is estimated from the measurement data $\mathbf{x}(\theta_{calj})$ by picking out the principal eigenvector of the covariance matrix of $\mathbf{x}(\theta_{calj})$. These steering vectors characterize the array.

In this paper both local [1] and global calibration [2] will be used. In both cases a correction matrix is calculated as the optimal matrix in a (weighted) least-square sense according to

$$\hat{\mathbf{Q}} = \arg\min_{\mathbf{Q}} \|(\mathbf{A_{meas}}(\boldsymbol{\theta}_{cal}) - \mathbf{Q}\mathbf{A}(\boldsymbol{\theta}_{cal}))\mathbf{W^{1/2}}\|_F, \quad (5)$$

where the subscript F means Frobenius norm, $\mathbf{W}$ is a weight matrix and $\boldsymbol{\theta}_{cal}$ is the vector of calibration angles. In the global case, the matrix $\mathbf{W}$ is the identity matrix and $\hat{\mathbf{Q}}$ is scan independent. Only one, full, matrix is calculated for all values of θ. In the local case the weight matrix $\mathbf{W}(\theta)$ is scan dependent, and one $\hat{\mathbf{Q}}(\theta)$ is calculated for each θ of interest. Since each correction matrix $\hat{\mathbf{Q}}(\theta)$ is calculated for a single direction θ, only a diagonal matrix $\hat{\mathbf{Q}}(\theta)$ is needed in the local case. The weighting matrix is also chosen to be diagonal. The diagonal elements (the solution to (5)) are then given by

$$\hat{q}_i(\theta) = \frac{\sum_{j=1}^{J} \mathbf{A}_{ij}^* w_j(\theta) \mathbf{A}_{\mathbf{meas}\,ij}}{\sum_{j=1}^{J} \mathbf{A}_{ij}^* w_j(\theta) \mathbf{A}_{ij}}, \quad (6)$$

where $w_j(\theta)$ denotes diagonal element j of the weighting matrix $\mathbf{W}(\theta)$. The weights $w_j(\theta)$ should give calibration data for angles θ_{calj} close to θ high weight. In this paper

$$w_j(\theta) = \exp(-hD_j^2), \quad (7)$$

defines the weights, and $D_j = |\theta_{calj} - \theta|$. Also other weight functions used [3] and [4, ch. 2] but as stated by the latter the choice of the parameter h is more important for the performance than the choice of weight function. The parameter h has the important role of determining the width of the weight function. A too narrow weight function will give a poorer interpolation between the calibration angles and poorer reduction of noise influence. A too broad weight function, on the other hand, will give a DOA estimate which is too much influenced by the scan dependent model errors. The angular bandwidth parameter h has been calculated from the calibration angles using a leave-one-out approach, see [5].

3. INTERPOLATE NEW CALIBRATION STEERING VECTORS

One problem with the global calibration method is that it requires a rather dense calibration grid, especially for large arrays. In the calculation of the correction matrix for the global method, using (5), it is required that $\mathbf{A}\mathbf{A}^*$ has full rank. This means that the number of calibration angles must be at least as many as the number of elements, i. e. $J \geq m$, with equal sign if all columns of $\mathbf{A}$ are orthogonal. The columns of $\mathbf{A}$ become orthogonal if $J = m$ and the calibration grid is chosen equidistant in $u = \sin\theta$. For a large array, it might be unfeasible or too expensive to do enough measurements. A remedy, in such a case, is to calculate intermediate calibration values by interpolating from the measured calibration data using local models. This makes it possible to use global calibration, even if the number of measured calibration angles are to few.

The calibration measurements are made in a sparse calibration grid $\boldsymbol{\theta}_{cal} = [\theta_{cal_1}, \ldots, \theta_{cal_j}, \ldots, \theta_{cal_J}]$, where $J < m$. The interpolation is when done like this:

I Chose the density of the pseudo calibration grid,

$$\boldsymbol{\theta}_{newcal} = [\theta_{newcal_1}, \ldots, \theta_{newcal_o}, \ldots, \theta_{newcal_O}] \quad (8)$$

where $O \geq m$, and $\theta_{newcal_1} = \theta_{cal_1}$ and $\theta_{newcal_O} = \theta_{cal_J}$.

II For each θ_{newcal_o}, calculate a local correction matrix, $\hat{\mathbf{Q}}(\theta_{newcal_o})$, using (6).

III The pseudo calibration measurements are given by

$$\mathbf{a}_{pseudomeas}(\theta_{newcal_o}) = \hat{\mathbf{Q}}(\theta_{newcal_o})\mathbf{a}(\theta_{newcal_o}). \quad (9)$$

for each $\theta_{cal_o} \in \boldsymbol{\theta}_{newcal}$

Finally the global correction matrix can be calculated from $\mathbf{A_{pseudomeas}}$.

4. ESPRIT WITH WEIGHTING

ESPRIT is a computationally efficient DOA estimation method which have the benefit that the DOA:s are given by numerical values rather than as peaks in a spatial spectrum, like conventional beam-forming or MUSIC. ESPRIT is usually applied to uniform linear arrays. Following [6], the second to nth row of the steering matrix $\mathbf{A}$, called $\mathbf{A_2}$, is given by

$$\mathbf{A_2} = \mathbf{A_1}\boldsymbol{\Phi}, \quad (10)$$

where $\mathbf{A_1}$ is the $n-1$ first rows of $\mathbf{A}$ and $\boldsymbol{\Phi} = \text{diag}([e^{jk\Delta\sin(\theta_1)}, \ldots, e^{jk\Delta\sin(\theta_d)}])$. The DOA:s are now a function of the eigenvalues of $\boldsymbol{\Phi}$ which can be estimated by using $\mathbf{E} = \mathbf{AT}$, where $\mathbf{E}$ is the d principal (signal) eigenvectors of the covariance matrix of the data $\mathbf{R}$ and $\mathbf{T}$ is a full rank matrix. Rewriting (10) as

$$\mathbf{E_2} = \mathbf{E_1}\mathbf{T^{-1}}\boldsymbol{\Phi}\mathbf{T} = \mathbf{E_1}\boldsymbol{\Psi}, \quad (11)$$

where $\mathbf{E}_1$ and $\mathbf{E}_2$ are defined conformably with $\mathbf{A}_1$ and $\mathbf{A}_2$, the eigenvalues of $\boldsymbol{\Phi}$ are now the same as the eigenvalues of $\boldsymbol{\Psi}$. The matrix $\boldsymbol{\Psi}$ is estimated by solving (11) in a least-squares sense.

When the actual array is not a ULA, the DOA estimation can be done on a virtual ULA by calibration, [7]. Virtual array means that the array data has been filtered to be like that from a ULA. This means that the relation between $\mathbf{A}$ and $\mathbf{E}$ is rewritten as

$$\mathbf{E} = \mathbf{QAT} \Rightarrow \mathbf{Q^{-1}E} = \mathbf{AT}. \quad (12)$$

In accommodating ESPRIT to local calibration two problems arise. The first is that the weighting of the calibration data depends on the unknown true DOA, and the second is that, even though there might be more than one source, the calibration data can, in the described procedure above, only be weighted after one DOA at the time.

The above complications can be met by a two-step procedure, which we will call two-step ESPRIT. In the first step a DOA estimation using a global correction matrix in (12) is done. The estimated DOAs are then used to weight the data in a second step, and the DOAs are estimated using ESPRIT, including a local correction matrix in (12). In the second step one set of weights and a diagonal correction matrix is calculated for each of the estimated DOAs. All the DOAs are estimated for each correction matrix, but only the DOA for which the weights was calculated is saved. The DOAs not weighted after are a potential source of bias error, but as will be shown in Section 5.3 the results from the two-step ESPRIT are still better than the globally calibrated estimation, which are biased by the scan dependent errors.

5. EXAMPLES

5.1. Simulated data

Array data containing position errors have been simulated using the function

$$\mathbf{x}(t) = \mathbf{DCA}(\boldsymbol{\theta})\mathbf{s}(t) + \boldsymbol{\eta}(t), \quad (13)$$

Table 1. The mean of the absolute value of the estimation error of the DOA of three sources (in degrees). The mean is calculated over 1000 simulations using different position and channel errors.

Source	No cal	Dense	Sparse 1	Sparse 2
$-20°$	0.80	0.44	0.42	0.11
-4 to $+55°$	3.2	1.1	0.97	0.95
1 to $+60°$	2.3	0.95	0.82	0.81

where $\mathbf{C}$ is a mutual coupling matrix, $\mathbf{D}$ is a diagonal matrix modelling channel errors as complex white gaussian noise with standard deviation 0.5, $\boldsymbol{\eta}$ is additive white gaussian noise in the receiver channels having unit standard deviation and the signals $\mathbf{s}(t)$ are 20dB above the noise $\boldsymbol{\eta}$. The steering vector $\mathbf{a}(\theta)$ has been modified to include positional errors

$$\mathbf{a}(\theta) = [1, e^{j\Delta k \sin(\theta)(1+\varepsilon_1)}, ..., e^{j\Delta k \sin(\theta)(m-1+\varepsilon_{m-1})}]^T \quad (14)$$

with random positional errors evenly distributed between -0.05λ and 0.05λ in the direction along the array. The element separation Δ is chosen to be 0.5λ. The array is assumed to be an $m = 8$ element array of thin half wavelength long dipoles with mutual impedance given by [8, p. 451]. If $\mathbf{Z}$ is a symmetric Toeplitz matrix with the mutual impedances, $\mathbf{I}$ is the identity matrix, Z_{self} is the self impedance and Z_c is the characteristic impedance of the feeding lines, the coupling matrix is given by $\mathbf{C} = (Z_{self} + Z_c)(Z_c\mathbf{I} + \mathbf{Z})^{-1}$. Conjugate match $Z_c = Z^*_{self}$ is used.

5.2. Interpolated new calibration data

The method to calculate new calibration data using local models will now be tested and evaluated using ESPRIT with global calibration. The DOAs for three sources are estimated. One source is fixed at $-20°$, one source moves from $0°$ to $90°$ and the last source moves from $-4°$ to $85°$. Four different calibration cases are tested. In all cases the (pseudo) calibration angles are spread equidistantly in $u = \sin(\theta)$ from $u = -1$ to $u = 1$. The cases are:

No cal no calibration

Dense cal global calibration with a measured calibration grid with $m + 1$ calibration angles

Sparse cal 1 global calibration with $m + 1$ pseudo calibration angles interpolated using local models from a measured calibration grid with $m/2 + 1$ calibration angles

Sparse cal 2 global calibration with $4m + 1$ pseudo calibration angles interpolated using local models from a measured calibration grid with $m/2 + 1$ calibration angles

Figure 1 shows the average of the DOA estimation errors (bias) in the estimation of the source moving from $0°$ to $90°$, calculated as an average of 1000 simulations with different position and channel errors. The dense calibration and the sparse calibration 1 have the same density in the (pseudo) calibration grid and performs almost the same, even if the sparse calibration 1 has only half the number of measured calibration angles. The sparse calibration 2 has four times as many (pseudo) calibration angles as the dense and the sparse calibration 1, and shows a result where the errors are smeared out over the DOAs. The case without calibration shows the worst performance.

Table 1 shows the mean of the absolute value of the estimation errors of the DOAs for all three sources. The average is only calculated over the region where the outermost source is not more than

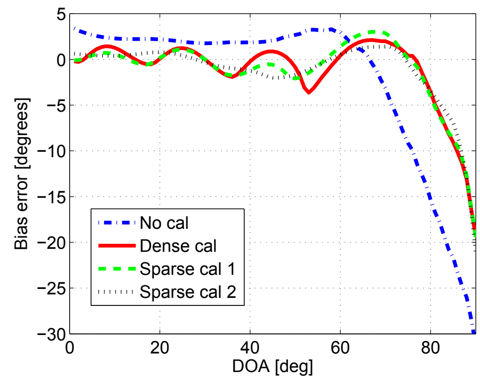

Fig. 1. Bias in DOA estimation of one of three sources, the third source in Table 1, using ESPRIT. The source is moving from $0°$ to $90°$, and the bias is calculated as an average of 1000 simulations with different position and channel errors.

$60°$ from broadside, even if Figure 1 indicates that the DOA estimation performs rather well out to almost $80°$ from broadside if calibration is used. The calibration using a measured sparse grid and local models to make the grid more dense shows at least as good results as using the measured dense calibration grid. The result is in some cases even better if the calibration grid is made even more dense (Sparse cal 2) using local models. We can conclude that it is possible to measure less calibration angles than the number of antenna elements, and still get the same or better performance if we calculate additional calibration angles from the measured ones using local models. This makes it possible to keep down the calibration grid density, which can be of major importance since calibration time can be very expensive. The calculations will, however, still be as heavy as if a measured dense calibration grid had been used.

5.3. Two-step ESPRIT

The two-step ESPRIT will be demonstrated on data from (13). The calibration data is taken every tenth degree, within $\pm 60°$. The validation data has three sources, one fixed at $23°$ and the other two moving, from $-1°$ to $-60°$ and from $1°$ to $-58°$ respectively. Fig. 2 shows the bias errors of the DOA estimates of the two moving sources calculated as a mean of 1000 trials with different noise, channel and position errors. In Table 2, the mean of the absolute value of the bias errors and the mean of the standard deviations of the estimates for all three sources are shown. It can be concluded what the two-step ESPRIT can improve both bias and variance errors compared to using only the global ESPRIT.

The method will also be demonstrated on measurement data from an ultrasound array testbed. The test setup consists of two loudspeakers which can be moved on a horizontal bar and an array of 8 microphones. As calibration data, measurements every degree between $-15°$ and $15°$ have been used. The validation data is single source measurements which are made at the same angles but at another time than the calibration data. This array is very far from being a ULA, since it has been bent, and the element accuracy is very poor. The maximal error perpendicular to the plane of the array is about one wavelength, and the DOA estimation using this array is therefore difficult.

This example demonstrates what happens if the data quality is

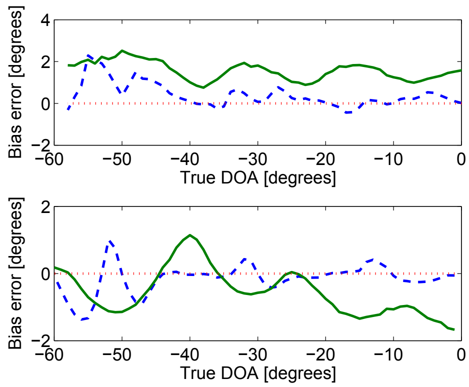

Fig. 2. Two sources moving, one from -58° to 1° (upper figure) and one from -60° to -1° (lower figure). The figures show the bias error in the DOA estimates as a function of the true value of the DOA for ESPRIT with global calibration (full line) and the two-step ESPRIT (dashed line).

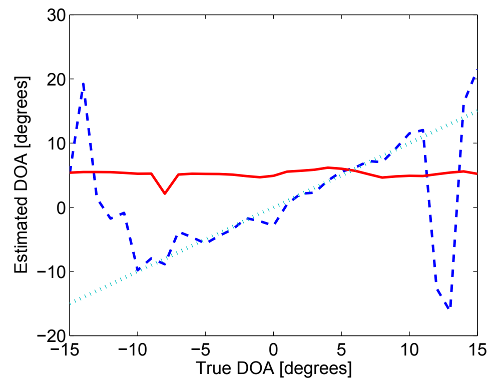

Fig. 3. Estimated DOA as a function of the true DOA using measured data from an ultrasound array testbed. Globally calibrated ESPRIT estimate (full line), locally calibrated multi-step estimate (dashed line) and true DOA (dotted line).

too poor. As can be seen in Figure 3, the global calibration completely fails to estimate the true DOAs. This estimate is, of course, too poor to be used as a start value for the two-step ESPRIT. One solution to this problem is to use an iterative procedure, where, the start value of the kth iteration is $\theta_k = 0.75\theta_{k-1} + 0.25\theta_{k-2}$ instead of just θ_{k-1}, to stabilize the convergence of the iterations. Figure 3 shows that this multi-step ESPRIT gives an acceptable result, close to broadside. It should be noted that the iterative estimation is not to recommend if it is not necessary, since convergence can not be guaranteed.

6. CONCLUSION

We have shown that for globally calibrated ESPRIT the performance can be kept while reducing the number of calibration measurements. This is achieved by calculating new calibration data from the calibration measurements using local calibration. This method offers a great possibility to reduce calibration time and cost, especially for large arrays. Furthermore, it is shown that adding a second step, involving local calibration to the ESPRIT estimation, can improve the performance in the presence of scan dependent errors in the array. An interesting extension of the research would be to see if treating the signals not weighted after as jammers could further improve the performance.

Table 2. The average of the absolute value of the bias and the average of the standard deviation of the DOAs of three sources (in degrees)

Average absolute value of the bias

Source	Two-step	Global
23°	0.0336	0.1329
1 to -58°	0.6949	1.6236
-1 to -60°	0.4551	0.8802

Average standard deviation

Source	Two-step	Global
23°	0.5183	0.6591
1 to -58°	1.4279	1.6387
-1 to -60°	1.0007	1.2178

7. REFERENCES

[1] A. Lundgren, M. Lanne and M. Viberg, “Array calibration using local models”, *Antenn 06, Nordic Antenna Symposium*, Linköping, Sweden, May-June, 2006, pp. 251-256.

[2] J. Pierre and M. Kaveh, “Experimental performance of calibration and direction-finding algorithms”, *IEEE Int. Conf. Acoust., Speech, Signal Processing*, Toronto, Canada, May, 1991, Vol. 2, pp. 1365-1368.

[3] C.G. Atkeson, A.W. Moore and S. Schaal, “Locally weighted learning”, *Artificial Intelligence Review*, Vol. 11, pp. 11-73, 1997.

[4] M.P. Wand and M.C. Jones, “Kernel smoothing”, *Chapman and Hall*, 1997.

[5] M. Lanne, A. Lundgren and M. Viberg, “Calibrating an array antenna for scan dependent errors using a sparse grid”, *Asilomar conference on Systems, Signals and Computers*, Asilomar, CA, Oct 29-Nov 1, 2006

[6] R. Roy, A. Paulraj and T. Kailath, “ESPRIT-A subspace rotation approach to estimation of parameters of cisoids in noise”, *IEEE Trans. on Accoustics, Speech and Signal processing*, Vol. 34, pp. 1340-1342, 1986.

[7] B. Friedlander and A.J. Weiss, “Direction finding for wideband signals using an interpolated array”, *IEEE Trans. on Signal Processing*, Vol. 41, pp. 1618-1634, April 1993.

[8] J.D. Kraus and R.J. Marhefka, “Antennas: For all applications”, *McGraw-Hill*, Third edition, 2002.